

SURFACE AND VOLUME REGISTRATION OF BRAIN MAGNETIC RESONANCE IMAGES

Natasha Lepore¹, Anand A. Joshi¹, Richard Leahy², Caroline Brun¹, Yi-Yu Chou¹, Xavier Pennec³,
Agatha D. Lee¹, Marina Barysheva¹, Greig I. de Zubicaray⁴, Margaret Wright⁵, Katie McMahon⁴,
Arthur W. Toga¹, Paul M. Thompson¹

¹ Laboratory of Neuro Imaging, UCLA School of Medicine, Los Angeles, CA, USA

² Department of Electrical Engineering, University of Southern California, Los Angeles, CA, USA

³ INRIA Sophia - Asclepios Project, Sophia Antipolis, France

⁴ Centre for Magnetic Resonance, University of Queensland, Brisbane, Australia

⁵ Genetic Epidemiology Lab, Queensland Institute of Medical Research, Australia

ABSTRACT

3D volumetric registration of brain images is particularly challenging in cortical regions due to their high complexity and folding. Here we develop a new combined algorithm for surface and volume registration of brain MR images. Our method proceeds in 3 steps: First, we segment the cortices and use the Freesurfer registration algorithm to obtain a map between cortical surfaces. This matching is extended to the whole brain volume by computing an harmonic map between the brain manifolds such that their surfaces remain aligned. Finally, the registered images from the first two steps are used as input to a 3D Riemannian fluid algorithm in order to obtain an accurate matching of the subcortical structures. The results show significant improvement over using fluid registration alone.

Index Terms— brain, image analysis, Magnetic Resonance Imaging, image registration

1. INTRODUCTION

The accurate non-linear matching of brain images is of great importance in medical imaging and neuroscience. Applications include the alignment of images from different subjects, time points or modalities, the comparison of brain anatomy between healthy and diseased populations, brain growth in childhood and adolescence [22] and genetic influences on brain structure [23].

Non-linear image registration consists of deforming a template image T to match a study image S . Typically, a displacement vector field $\vec{u}(\vec{r})$ is found such that $|T(\vec{r} - \vec{u}) - S(\vec{r})|$ is minimized, thus aligning geometrical features of the images. Here r is the voxel location. The anatomical correspondence between images is determined either from intensity-based comparisons between the images, for instance the mean square intensity difference between images, or mutual information, or from common features such as anatomical landmarks. These correspondences are used to

drive the registration. At the same time, a regularizer is used to constrain the transformation and ensure that the deformation is smooth, or has several desirable properties that may be required by the problem at hand such as inverse-consistency, or invertibility.

One common way to select a regularizer is to assign a continuum mechanical law to the deforming image medium. For instance, in elastic registration [8], the image is regarded as embedded in an elastic medium. A force is applied based on the chosen similarity function that pulls the template into agreement with the study, while elastic forces attempt to restore it to its original shape. Elastic registration works very well in cases where small deformations are needed, for instance in longitudinal studies where the same subject is compared at two time points and only small changes are expected. However, large deformations can induce shearing or tearing of the elastic medium. As a result, when there are substantial differences between the two images, other methods are used instead. In fluid registration [6], for instance, the image is treated as embedded in a viscous fluid that follows a linearized version of the Navier-Stokes equation, with a velocity field that is the time derivative of the deformation field $\vec{v}(\vec{r}, t) = \frac{d\vec{u}(\vec{r}, t)}{dt}$. The template image is flowed onto the study image, while the driving force is again generated from a similarity function. The fluid flow allows large deformations without shearing or tearing the image.

More recently, in [17], a new elastic regularizer was proposed. The regularization is done on the matrices $\Sigma = (\nabla \vec{u} + I)^T (\nabla \vec{u} + I)$, which characterize the local changes in shape and volume due to the registration. Here I is the identity matrix. As the Σ 's are positive-definite symmetric matrices, the computations are performed in the Log-Euclidean framework [1], which allows analytical computations on the manifold of Σ 's. We developed a fluid version of this method in [5], where the rate of change of Σ was regularized instead.

However, algorithms such as fluid registration that attempt to register whole brain volumes usually give poor results on the cortex, due to the high complexity and variability

ity of cortical surfaces. Thus, when good cortical registration is required, comparisons are often made by segmenting them and matching the segmented surfaces. The registrations are generally performed by first transforming the cortical surfaces to some intermediate and more regular surface such as the plane or sphere, though some recent algorithms have been developed to register the cortical surfaces directly [20]. Typically, sets of sulci or gyri are that are common to all normal brains are used as landmarks to guide the transformation [23].

In [11], a new algorithm was designed that combines both surface and volume registrations. First, the cortical surfaces are parametrized and aligned using traced sulci as landmarks. A constrained harmonic mapping is then used to extend this correspondence to the whole brain volume. Finally, an elastic registration is performed to align the subcortical structures.

The algorithm in [11] gives very accurate matching near the cortex. However, as the volume registration uses an elastic regularizer, it is not ideal for matching subcortical structures when large deformations are needed. Here we improve on the algorithm in [11] by substituting the elastic volume registration with the Riemannian fluid algorithm from [5]. More formally, our combined algorithm addresses the following problem: produce a one-to-one mapping between two brain volumes such that (1) subcortical structures and sulcal landmarks are aligned and (2) there is also a smooth one-to-one correspondence between the cortical surfaces of the two volumes. Equivalently, given 3D manifolds M and N representing the two brain volumes, with boundaries ∂M and ∂N representing their respective cortical surfaces, we find a map from M to N such that ∂M , the surface of M , maps to ∂N , the surface of N , and the intensities of the images in the interior of M and N are matched as far as possible. In addition, the map satisfies a surface matching constraint so that the surface ∂M maps onto ∂N . The boundaries, ∂M and ∂N , are assumed to have a spherical topology.

We validate our new combined algorithm using MR images from healthy control adult subjects.

2. METHOD

2.1. Surface-Volume registration

Intensity-based volume registration methods can align subcortical structures well, but the variability in sulcal folding patterns typically results in misalignment of the cortical surface. Conversely, surface-based registration using sulcal features can produce excellent cortical alignment but the mapping between brains is restricted to the cortical surface. The algorithm in [11] uses sulci as landmarks for cortical registration. However, for large data sets, this method is prohibitive as the landmarks need to be hand traced. Here instead, we used Freesurfer [7] to perform the alignment of the cortical surfaces. The registration was done to another subject from the same dataset for which the cortex was extracted to serve

as the target surface. We then use a constrained harmonic mapping from [11] to extend this surface correspondence to the entire cortical volume.

We solve the mapping problem in three steps:

1. Surface matching, which computes a map between ∂M and ∂N , the cortical surfaces of the two brains. We used Freesurfer to perform this alignment.
2. Extrapolation of the surface map to the entire enclosed cerebral volume such that the cortical surfaces remain aligned. This is done by computing a harmonic map u from M to N with a surface matching constraint. The map is computed using an intermediate unit ball space. Let $h_{\alpha\beta}$ denote the metric of N associated with the unit ball mapping of N . Then the harmonic map $u : M \rightarrow N$ can be computed by minimizing the mapping energy:

$$E(u) = \frac{1}{2} \int_M \sum_{i,j=1}^3 \sum_{\alpha,\beta=1}^3 h_{\alpha\beta}(u(x)) \frac{\partial u^\alpha(x)}{\partial x^i} \frac{\partial u^\beta(x)}{\partial x^j} d\mu_g, \quad (1)$$

The harmonic map u computed by minimizing the mapping energy defines a diffeomorphism between subject and target volumes such that the sulcal folding patterns register. The details of this method are described in [11]

3. Refinement of the harmonic map on the interiors of M and N to improve intensity alignment of subcortical structures. For this we use the Riemannian fluid approach described in [5]. An outline of the method is described in the following section.

2.2. Volume registration

In fluid registration, the matching is performed in a series of time steps, dt . The velocity $\vec{v}(\vec{x}, t)$ (the time derivative of the displacement field $\vec{u} = d\vec{v}/dt$) is computed at each time t and voxel \vec{x} from:

$$\frac{d\vec{v}(\vec{x}, t)}{dt} = \nabla Cost + \nabla Reg(\vec{v}, t) - v \quad (2)$$

where $Cost$ denotes the similarity cost function and Reg is the regularizer. \vec{v} is integrated over time to obtain the final displacement field \vec{u} .

In Riemannian fluid registration, the regularization is performed on the matrix logarithm of the rate of strain $\Sigma_v = (\nabla\vec{v} + I)^T(\nabla\vec{v} + I)$:

$$Reg_{Riem}(\vec{v}, t) = \int \frac{\mu}{4} Tr(\log(\Sigma_v^2)) + \frac{\lambda}{8} Tr(\log(\Sigma_v))^2. \quad (3)$$

The coefficients μ and λ are the parameters of the fluid (similar to the Lamé coefficients) and are chosen by the user.

Reg_{Riem} is the fluid equivalent of the Riemannian elastic regularizer from [17], which is found by replacing Σ_v by Σ in Eq. 2. The deformation tensors $\Sigma = (\nabla \vec{u} + I)^T (\nabla \vec{u} + I)$ characterize the local shape and volume deformation. These tensors live on the curved manifold of positive-definite, symmetric matrices. Taking the matrix logarithm of Σ transports it to the tangent plane at the origin of the manifold, which is a flat space in which simple computations can be performed [1].

We chose an intensity-based similarity measure, that is, the gradient of the difference in intensity between the template T and the study S :

$$\nabla Cost(\vec{x}, \vec{u}(\vec{x}, t)) = -[T(\vec{x} - \vec{u}(\vec{x}, t)) - S(\vec{x})] \nabla T|_{\vec{x} - \vec{u}(\vec{x}, t)}$$

Details of the implementation may be found in [5].

2.3. Data

We used a dataset of MR images from healthy adult subjects. Our images were collected using a 4 Tesla Bruker Medspec whole body scanner (Bruker Medical, Ettingen, Germany) at the Center for Magnetic Resonance (University of Queensland, Australia). Three-dimensional $T1$ -weighted images were acquired with a magnetization prepared rapid gradient echo (*MP-RAGE*) sequence to resolve anatomy at high resolution. Acquisition parameters were: inversion time (TI) / repetition time (TR) / echo time (TE) = 1500 / 2500 / 3.83 msec; flip angle = 15° ; slice thickness = 0.9 mm with a 256x256x256 acquisition matrix.

Extracerebral (non-brain) tissues were manually deleted from the MRI images using the 3D interactive program Display (Montreal Neurological Institute, McGill University, Canada). All scans were then aligned to the ICBM53 template using 9-parameter registration (i.e., translational and rotational alignment, allowing scaling in 3 independent directions) found in the *FMRIB's* Linear Image Registration Toolbox, *FLIRT* [10].

2.4. Non-linear Registration

For each image in the data set, we obtained an initial displacement field \vec{u}_0 , and an initial registered image from the harmonic mapping algorithm described in sec. 2.1. The registered image was used as input for the 3D Riemannian fluid algorithm from sec. 2.2. The final displacement field was obtained by concatenating the displacements from the surface and 3D non-linear registration steps. In our implementation, the final displacements were computed from the common template to each image in the data set, while the registered image was the result of transforming each subject into the template, thus allowing all comparisons to be made in the common space.

3. RESULTS

In **Fig.1**, we compare the results of our combined registration algorithm with those of using the Riemannian fluid registration alone, without surface constraints. Subcortical regions are well registered with both algorithms. However, the combined algorithm far outperforms the 3D Riemannian registration in cortical areas.

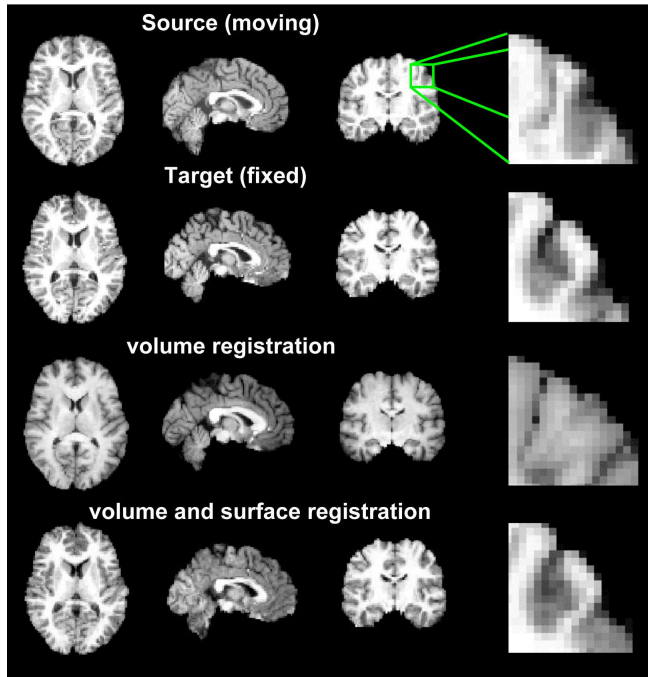


Fig. 1. Comparison of the results of the combined algorithm to those of the 3D Riemannian algorithm with no surface constraints. Registration results are shown mapping one subject to a template for sagittal (left column), coronal (middle column) and horizontal (right column) slices. The top row is the moving image and the second row the fixed target image. The last two rows show the results of the registration for the volumetric (third row) and combined (fourth row) algorithms; the fourth row shows accurate cortical and subcortical registration.

4. DISCUSSION

We investigated the a new combined algorithm for the registration of brain MR images. Our algorithm was tested on a data set of MZ and DZ twins, and showed significant improvement over using fluid registration alone, particularly in the vicinity of the cortex.

There are several ways to achieve a good registration over the whole brain volume, including the cortical surface. The simplest one, which we investigated here, is to use a cortical surface registration to obtain an initialization for a 3D regis-

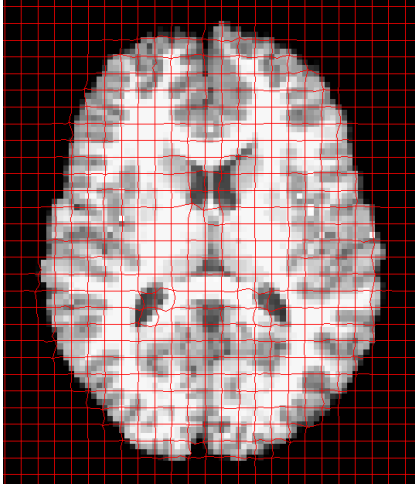


Fig. 2. Deformation of a regular grid from the registration

tration. In that case, as we showed here, the matching converges to better local minimum compared to the one found from the fluid registration alone. However, as the cortex is allowed to move during the fluid registration, it can potentially reduce the accuracy of the matching found from the cortical matching algorithm. Thus, as an alternative, one could choose instead to re-introduce the cost function from the first cortical matching algorithm into the volume registration, either as a hard constraint or with a Lagrange multiplier. As the matching was already quite good with the first method, this second method was not pursued here, though it would be an interesting extension of this work. Finally, in cases where both the above methods fail, a third option would be to force the displacements from the Riemannian fluid algorithm to match those found from the cortical mapping.

Acknowledgments

This work was generously supported by NIH grant R01 HD050735 and the National Health and Medical Research Council, Australia grant 496682.

5. REFERENCES

- [1] Arsigny V, et al., *Mag Res Med* 56, (2006) 411-421.
- [2] Ashburner J, *Neuroimage* 38, (2007) 95-113.
- [3] Brun C, et al., *Workshop on Statistical Registration: Pair-wise and Group-wise alignment and atlas formation*, MICCAI (2007).
- [4] Brun C, et al., *ISBI* (2008).
- [5] Brun C, et al., *MICCAI* (2008).
- [6] Christensen GE, Rabbitt RD, Miller MI, *IEEE Trans Imag Process* 5, (1996) 1435-1447.
- [7] Dale A M, Fischl B, *Neuroimage* 9, (1999) 179-94.
- [8] Davatzikos C, et al., *J Comp Assist Tomogr* 20, (1996) 88-97.
- [9] Gramkow C, Master's thesis, Danish Technical University, Copenhagen, Denmark (1996).
- [10] Jenkinson M, et al., *Neuroimage* 17, (2002) 825-841.
- [11] Joshi AA, et al., *IEEE Trans Med Imag* 26, (2007) 1657-1669.
- [12] Leporé N, et al., *MICCAI* (2007).
- [13] Leporé N, et al., *IEEE Trans Med Imag* 27, (2008) 129-141.
- [14] Lepore N, et al., *SPIE conference on Physiology, Function and Structure from Medical Images* (2008).
- [15] Lepore N, et al., *ISBI* (2008).
- [16] Nichols TE, Holmes AP, *Hum Brain Map* 15, (2001) 1-25.
- [17] Pennec X, et al., *MICCAI* (2005) 943-950.
- [18] Scout PE, Fleiss JL, *Psychol Bull* 2, (1979) 420-428.
- [19] Shattuck DW and Leahy RM, *Med Imag Anal* 8, (2002) 129-141.
- [20] Shi Y, et al., *Med Imag Anal* 11, (2007) 207-223.
- [21] Storey JD, *J Roy Stat Soc B* 64, (2002) 479-498.
- [22] Thompson PM, et al., *Nature* 404, (2000) 190-193.
- [23] Thompson PM, et al., *Nat Neurosci* 4, (2001) 1253-1258.